



Smith, G., Kemp, R., Pegg, J. C., Rogers, S. E., & Eastoe, J. (2015). Sulfosuccinate and Sulfocarboxylate Surfactants As Charge Control Additives in Nonpolar Solvents. *Langmuir*, 31(51), 13690-13699. <https://doi.org/10.1021/acs.langmuir.5b03876>

Peer reviewed version

License (if available):  
CC BY-NC

Link to published version (if available):  
[10.1021/acs.langmuir.5b03876](https://doi.org/10.1021/acs.langmuir.5b03876)

[Link to publication record in Explore Bristol Research](#)  
PDF-document

This is the author accepted manuscript (AAM). The final published version (version of record) is available online via ACS at <http://pubs.acs.org/doi/10.1021/acs.langmuir.5b03876>. Please refer to any applicable terms of use of the publisher.

## University of Bristol - Explore Bristol Research

### General rights

This document is made available in accordance with publisher policies. Please cite only the published version using the reference above. Full terms of use are available: <http://www.bristol.ac.uk/red/research-policy/pure/user-guides/ebr-terms/>

# Sulfosuccinate and sulfocarboxylate surfactants as charge control additives in nonpolar solvents

Gregory N. Smith,<sup>†,‡</sup> Roger Kemp,<sup>¶,§</sup> Jonathan C. Pegg,<sup>†</sup> Sarah E. Rogers,<sup>||</sup> and  
Julian Eastoe<sup>\*,†</sup>

<sup>†</sup>*School of Chemistry, University of Bristol, Cantock's Close, Bristol, BS8 1TS, United Kingdom*

<sup>‡</sup>*Current address: Department of Chemistry, University of Sheffield, Brook Hill, Sheffield, South Yorkshire, S3 7HF, United Kingdom*

<sup>¶</sup>*Merck Chemicals Ltd, University Parkway, Chilworth, Southampton, SO16 7QD, United Kingdom*

<sup>§</sup>*Current address: Battelle UK, Hampshire, PO9 1SA, United Kingdom*

<sup>||</sup>*ISIS-STFC, Rutherford Appleton Laboratory, Chilton, Oxon OX11 0QX, United Kingdom*

E-mail: julian.eastoe@bristol.ac.uk

## Abstract

A series of eight sodium sulfonic acid surfactants with differently branched tails (four double-chain sulfosuccinates and four triple-chain sulfocarboxylates) were studied as charging agents for sterically-stabilized poly(methyl methacrylate) (PMMA) latexes in dodecane. Tail branching was found to have no significant effect on the electrophoretic mobility of the latexes, but the number of tails was found to influence the electrophoretic mobility. Triple-chain, sulfocarboxylate surfactants were found to be more effective. Several possible origins of this observation were explored by comparing sodium dioctylsulfosuccinate (AOT1) and sodium trioctylsulfocarboxylate (TC1) using identical approaches: the inverse micelle size, the propensity for ion dissociation,

the electrical conductivity, the electrokinetic or  $\zeta$  potential, and contrast-variation small-angle neutron scattering. The most likely origin of the increased ability of TC1 to charge PMMA latexes is a larger number of inverse micelles. These experiments demonstrate a small molecular variation that can be made to influence the ability of surfactants to charge particles in nonpolar solvents, and modifying molecular structure is a promising approach to developing more effective charging agents.

## Introduction

Although surfactants are well-known as charging agents for particles in nonpolar solvents, few different types have been used as charge control additives in academic studies.<sup>1</sup> The surfactants studied so far are completely different molecules, and there have been few attempts in the literature at making systematic variations.<sup>2</sup> Given the importance of charging in non-aqueous solvents,<sup>3</sup> for applications as diverse as petroleum safety,<sup>4</sup> printer and photocopier toners,<sup>5</sup> and electrophoretic electronic paper displays,<sup>6,7</sup> there is a need for understanding how the structure of surfactant charging agents can be related to their effectiveness. In this paper, changes to the hydrophobic (or solvophilic) portion of the surfactant molecule will be considered.

Studies of water-in-oil microemulsions have shown connections between the structure of surfactant alkyl tails and their performance. Surfactants with linear chain tails cannot stabilize microemulsions without the addition of a co-surfactant. However, once some branching is introduced into the surfactant tails (enabling microemulsification of water), there is little difference between the interfacial behavior of the surfactants.<sup>8</sup> The number of surfactant tails also influences the ability of the surfactants to form microemulsions. Double-chain surfactants are well-known microemulsifiers.<sup>8</sup> Double- and triple-chain surfactants with the same tails have been designed to solubilize water in alkanes and supercritical CO<sub>2</sub>, two very nonpolar fluids.<sup>9,10</sup> However, the single-chain analogue of Aerosol OT (AOT) does not support water-in-oil microemulsions, and the triple-chain analogue of AOT only stabilizes a

small amount of water and forms polydisperse or binary structures.<sup>11</sup> This demonstrates the complicated relationship between branching/hydrophobicity and the performance of surfactants in nonpolar solvents.

Changing the number of surfactant tails varies the hydrophobicity and critical packing parameter ( $P_c$ ) of the molecules,<sup>12</sup> and consequently, their packing at interfaces. Gacek and Berg recently studied the conductivity and charging ability of nonionic Span surfactants as a function of their hydrophilic-lipophilic balance (*HLB*). Higher *HLB* surfactants give higher solution conductivities and higher magnitude charges on mineral oxide particles. This suggests a connection between surfactant structure and particle charge, at least for nonionic surfactants and mineral oxide particles.<sup>13</sup>

In this paper, the charging ability of branched surfactants with different numbers of tails (two or three) has been studied. Only branched-tail surfactants are studied as linear-tail ionic surfactants do not form water-in-oil microemulsions so are not active in alkane solvents. Differences are indeed found between the ability of these surfactants to charge sterically-stabilized poly(methyl methacrylate) (PMMA) latexes. Several origins of the differing charging abilities of the surfactants are explored. These include molecular properties (ion dissociation), aggregate properties (inverse micelle size and electrical conductivity), and latex properties ( $\zeta$  potential and surfactant-latex interaction). The relationship between surfactant structure and charging ability has revealed design approaches to producing highly active charge control additives (CCAs).

# Experimental

## Materials

### Surfactant charging agents

Sulfosuccinate (AOT headgroup) and sulfocarboxylate (TC headgroup) surfactants were synthesized using appropriate branched alcohol precursors. AOT1- $d_{34}$ , AOT4, AOT6, and TC4 were previously synthesized and were used after characterization.<sup>10,11,14</sup> Diester and triester precursors of the remaining surfactants were synthesized using fumaryl chloride (AOT2) or *trans*-aconitic acid (TC1, TC1- $d_{51}$ , TC2, and TC6). The esters were then sulfonated to produce a surfactant. Full details and analytical chemistry are provided in the Supporting Information.

### PMMA latexes

MC1 latexes were a gift from Merck Chemicals Ltd. and have a solvodynamic diameter of  $412 \pm 5$  nm with a polydispersity index (PdI) of 0.07 (Malvern ZetaSizer Nano S90). GS1 and SF1 latexes were prepared by a classic dispersion polymerization process using the method described by Antl *et al.*<sup>15</sup> The *Z*-average solvodynamic diameter of GS1 latexes was  $76.1 \pm 0.5$  nm with a PdI of 0.11 and of SF1 latexes was  $666 \pm 24$  nm with a PdI of 0.13, measured by DLS (Malvern ZetaSizer Nano S90).

## Methods

### Small-angle neutron scattering (SANS).

Neutron scattering measurements were performed at the ISIS Pulsed Neutron Source. On Sans2d, a simultaneous *Q*-range of 0.003–0.43 Å<sup>-1</sup> was achieved using an instrument set up with the source-sample and sample-detector distances of  $L_1=L_2=8$  m and the 1 m<sup>2</sup> detector offset vertically 60 mm and sideways -290 mm.<sup>16</sup> On LOQ, data were recorded on a single

two-dimensional detector to provide a simultaneous  $Q$ -range of 0.008–0.24 Å<sup>-1</sup> utilizing neutrons with  $2 \leq \lambda \leq 10$  Å.<sup>17</sup> The beam diameter was 8 mm. Raw scattering data sets were corrected for the detector efficiency, sample transmission and background scattering and converted to scattering cross-sections using the instrument-specific software, Mantid. These data were placed on an absolute scale (cm<sup>-1</sup>) using the scattering from a standard sample (a solid blend of hydrogenous and perdeuterated polystyrene).<sup>18</sup> Data have been fit to models as described in the text using the SasView small-angle scattering software package.

### **Phase-analysis light scattering (PALS)**

Electrophoretic mobilities were measured using a Malvern Zetasizer Nano Z or ZS with a universal dip cell electrode. The applied field strength used was either  $1.0 \times 10^4$  V m<sup>-1</sup> or  $2.0 \times 10^4$  V m<sup>-1</sup>, depending on the electrophoretic mobility of the sample being measured. The lowest field strength possible was used to avoid any effect of field dependent mobility.<sup>19</sup> Six runs of 50 measurements were performed, and the average of these runs was used.

### **Electrical conductivity**

Conductivities in nonpolar solvents were measured using a model 627 conductivity meter (Scientifica, Princeton, N.J.). The instrument consisted of a stainless steel cup probe that was fully immersed in the sample.

### **Computational chemistry**

Computational chemistry calculations were performed using Gaussian 09.<sup>20</sup> Geometry optimization was performed initially using DFT at the B3LYP/6-31+G(d) level of theory. As ions were being studied, it was important to include diffuse functions in the basis set. Molecular energies were calculated using DFT at the B3LYP/6-31+G(d) level of theory, and zero-point vibrational energies were also calculated using B3LYP/6-31+G(d). The vibrational energies were scaled according to literature.<sup>21</sup> Izgorodina *et al.* showed that DFT at

the B3LYP/6-31+G(d) level of theory was appropriate for the calculation of proton affinities.<sup>22</sup>

## Results

The sodium alkyl sulfate/sulfonate family of surfactants was chosen as a design motif. Within this surfactant type, it is simple to make small molecular variations to go from one chain to four chains, as shown in Table 1. Increasing the number of chains raises the value of the critical packing parameter  $P_c$  (also shown in Table 1); this influences the shapes of the aggregates the surfactants form.<sup>12,23</sup> The single-chain surfactant (sodium 2-ethylhexylsulfate, SC1) and the double-chain surfactant (sodium di-2-ethylhexylsulfosuccinate, AOT1) are commercially available. The triple-chain surfactant (sodium tri-2-ethylhexylsulfocarboxylate, TC1)<sup>11,24</sup> and the quadruple-chain surfactant (sodium  $N, N'$ -dioctyl- $N, N'$ -di-2-ethylhexyl-2-sulfosuccinamide, QC1)<sup>25</sup> have been reported in the literature. These surfactants have differing solubility in aliphatic organic solvents. AOT1 and TC1 are known to be highly soluble. SC1 is insoluble.<sup>11</sup> QC1 is only sparingly soluble ( $< 10$  mM) in heptane and isooctane.<sup>25</sup> Given the solubilities of the surfactants, only the double-chain and triple-chain surfactants were explored further.

Four branched tails were studied in both double-chain and triple-chain forms, shown in Table 2. [The synthesis of the surfactants is outlined in Scheme 1.](#) The tail groups were chosen to cover a range of degrees of branching, described by an empirical “branching factor” devised by Nave.<sup>29</sup> It accounts for both the length and the position of the branch.

In total, eight surfactants have been studied as charge control additives, two sets with the four tail groups shown in Table 2. Four are double-chain, equivalently sulfosuccinate, surfactants. As a group, they will be referred to as “AOTx” surfactants, given that they have the same general structure as commercial sodium di-2-ethylhexylsulfosuccinate or AOT. Four are triple-chain, equivalently sulfocarboxylate, surfactants. As a group, they will be referred

Table 1: Alkyl sulfates and sulfonates with different chain numbers.

Surfactant	$P_c^a$	Molecular structure
Sodium 2-ethylhexylsulfate (SC1)	0.55	
Sodium di-2-ethylhexylsulfosuccinate (AOT1)	0.71	
Sodium tri-2-ethylhexylsulfocarballate (TC1)	1.5	
Sodium <i>N, N'</i> -dioctyl- <i>N, N'</i> -di-2-ethylhexyl-2-sulfosuccinamide (QC1)	> 1.8	

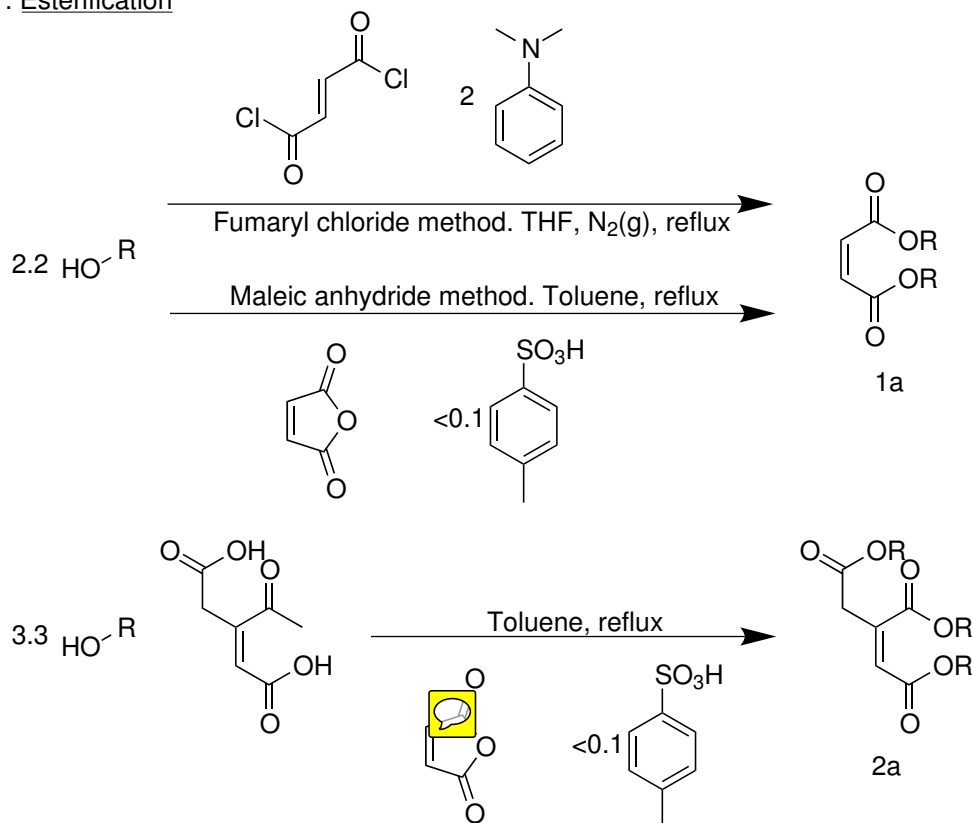
<sup>a</sup>  $P_c = v/(a_0 l_c)$ .  $v$  and  $l_c$  calculated according to literature.<sup>26,27</sup>  $a_0$  for AOT1 taken from literature,<sup>27,28</sup> SC1 and TC1 extrapolated from literature on SC4 and TC4,<sup>10</sup> QC1 set to value for TC1.

Table 2: Structure and branching factor of surfactant tails.

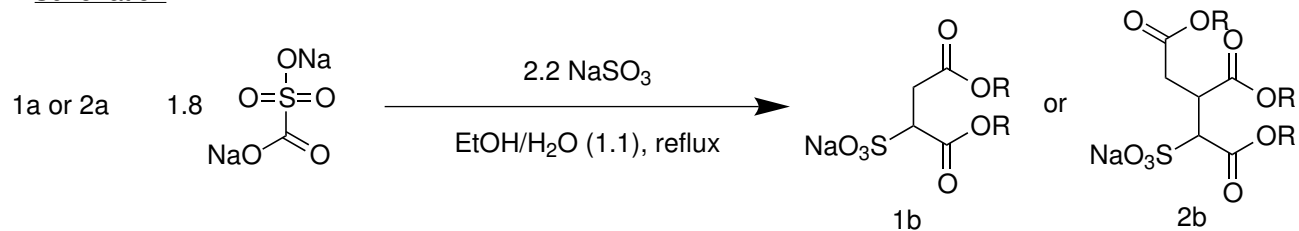
Tail Number	Branching factor	Molecular structure
1	$1.\bar{6}$	
2	2.4	
4	$1.\bar{3}$	
6	$1.\bar{3}$	



## 1. Esterification



## 2. Sulfonation



Scheme 1: Synthesis of sodium dialkylsulfosuccinate and trialkylsulfocarboxylate surfactants.

to as “TCx” surfactants, as they are “triple-chain” surfactants. This is the convention used for these types of surfactant molecules.<sup>8,28</sup>

## AOTx and TCx surfactants

### Electrophoretic mobility

The electrophoretic mobilities ( $\mu$ ) of PMMA latexes (MC1) charged by AOTx and TCx surfactants were measured using PALS. The volume fraction of particles was fixed ( $\phi = 5 \times 10^{-4}$ ), and the surfactant concentration was varied from 3–100 mM. The reduced electrophoretic mobilities ( $\mu/\mu_0$ , where  $\mu_0 = e/6\pi\eta\lambda_B$  and  $\lambda_B = e^2/4\pi\epsilon_0\epsilon_r k_B T$ , the Bjerrum length<sup>30</sup>) are shown rather than the raw experimental mobilities to normalize for the difference in solution viscosity, which is greater due to the presence of “hard sphere” surfactant inverse micelles. The relative viscosities for the solutions ( $\eta_r$ ) have been calculated using the Einstein relationship ( $\eta_r = 1 + 2.5 \cdot \phi$ ),<sup>31,32</sup> which has been shown to be appropriate for AOT solutions in dodecane.<sup>33</sup>

The reduced mobilities for AOTx and TCx charged latexes are shown in Figure 1. The many sets of data from all the surfactants overlap, making the difference between sulfosuccinates and sulfocarboxylates hard to see clearly. The shaded areas show the average mobilities for the two types of surfactants, and the filled areas indicate  $\pm 1$  standard deviation of the mean. Many measurements are shown (variations in concentration and surfactant tail), but there is only a weak effect of tail branching (charging decreases with increasing branching). There is no surfactant tail structure that is unequivocally the most effective at all concentrations. Therefore, changing tail branching does not seem a viable method to influence the charge of latexes.

From the shaded regions shown in Figure 1, it is apparent that TCx surfactants are more effective charge control additives than AOTx surfactants. At the highest concentrations, the data overlap within the error bars, although the mean  $\mu/\mu_0$  for TCx surfactants is still greater than the mean  $\mu/\mu_0$  for AOTx surfactants. As the surfactant concentration is

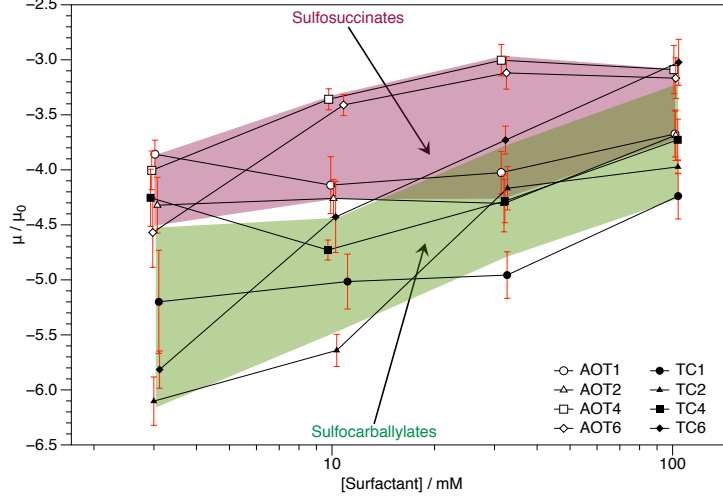



Figure 1: Reduced electrophoretic mobilities ( $\mu/\mu_0$ ) of PMMA latexes (MC1,  $\phi = 5 \times 10^{-4}$ ) charged by AOTx and TCx surfactants. Two shaded regions are shown, representing the average value of  $\mu/\mu_0$  for each type of surfactant (maroon - AOTx or sulfosuccinates, green - TCx or sulfocarboxylates) and filled in over  $\pm 1$  standard deviation. On average, the TCx surfactants are more effective charge control additives than the AOTx surfactants.

decreased, the magnitudes of the mobilities of TCx charged latexes increase more rapidly than for the AOTx charged latexes. TCx surfactants are clearly, on average, better charge control additives than AOTx surfactants. The origin of this increased effectiveness is not immediately clear, given the complexity of the system. Understanding the mechanism of increased charging ability would enable the production of more effective CCAs.

One possibility is inverse micelle (ion) size. The low relative permittivity of alkane solvents results in a correspondingly long Bjerrum length ( $\lambda_B$ ). The Bjerrum length represents the distance that two ions would need to be separated to ensure complete dissociation in a solvent. For dodecane,  $\lambda_B$  is 28 nm, and while this is much larger than the size of an AOT inverse micelle ( $r \approx 2$  nm),<sup>34</sup> the larger the inverse micelle counterion, the more likely particle charging would be. The size of inverse micelles can be measured using small-angle neutron scattering (SANS).


## ~~Small-angle neutron scattering~~ Inverse micelle size

The size of inverse micelles of all AOTx and TCx surfactants at a concentration of 10 mM in dodecane- $d_{26}$ . The raw data and fits are shown in the Supporting Information. The SANS curves are all qualitatively similar and can be fit to an idspherical form factor.<sup>35</sup> Therefore, all AOTx and TCx surfactants form small, spherical inverse micelles in dodecane. There is little difference in the size of the inverse micelles, and there are no significant differences between inverse micelles formed by corresponding AOTx and TCx surfactants within a standard error for SANS fitting ( $\pm 1$  Å). The TCx inverse micelles are slightly smaller than the AOTx micelles (by 3–18%), but this is not significant. Therefore, the size of inverse micelle counterions cannot explain the increased mobility of latexes charged by these surfactants.

Other possible explanations for the enhanced charging ability of TCx surfactants need to be explored. To simplify this analysis, only one pair of surfactants, AOT1 and TC1, will be considered further. This pair of surfactants was chosen for several reasons. AOT1 has been well-studied as both an electrolyte and as a CCA.<sup>1</sup> Additionally, the availability of deuterium-labeled 2-ethyl-1-hexanol- $d_{17}$  enables the synthesis of surfactants that can be used to obtain contrast in contrast variation-SANS (CV-SANS) experiments.<sup>14,36</sup>

## AOT1 and TC1 surfactants

The reduced mobilities ( $\mu/\mu_0$ ) of PMMA latexes charged by AOT1 and TC1 were shown in Figure 1. TC1 is a more effective charging additive at all concentrations than is AOT1. Double-chain AOT1 has been studied extensively as a charging agent for PMMA latexes in the literature,<sup>14,36–46</sup> but the triple-chain analogue TC1 has not been used as a charging agent previously. The two surfactants were explored using the same range of techniques to determine what controls their charging ability.

There are several possible reasons that TC1 surfactant could be a more effective charge control additive than AOT1. The orexplored in this paper are ~~listed below.~~ the inverse


micelle size, the degree of ion dissociation, the electrical conductivity, the electrokinetic ( $\zeta$ ) potential, and surfactant incorporation/absorption.

- ~~Inverse micelle size~~
- ~~Ion dissociation~~
- ~~Electrical conductivity~~
- ~~Electrokinetic ( $\zeta$ ) potential~~
- ~~Surfactant incorporation/absorption~~

Some relate to the inverse micelles, such as their size, dissociation, or conductivity, which can influence the mobility of the latexes as the inverse micelles act as counterions in the preferential adsorption mechanism.<sup>1</sup> Others relate to the particles, such as the  $\zeta$  potential or penetration by surfactant.

### **Inverse micelle size**

SANS measurements were performed on solutions of AOT1 and TC1 surfactants in dodecane- $d_{26}$  as a function of concentration, and the results are shown in in Figure 2. Even at the lowest concentrations, these samples are well above the CMC for inverse micelle formation in alkanes.<sup>47</sup>

The SANS curves have been fit to an ideal  spherical form factor.<sup>35</sup> The fit parameters are shown in Supporting Information. The fit values of the scale are consistent with the volume fractions from sample preparation, and the sizes of the inverse micelles of each surfactant at all concentrations are essentially the same. This agrees with the high-resolution SANS measurements used to measure CMCs for inverse micelle formation in cyclohexane.<sup>47</sup> The mean sizes of AOT1 and TC1 inverse micelles are slightly different. AOT1 inverse micelles on average have a radius of  $\sim 16$  Å, and TC1 inverse micelles on average have a radius of

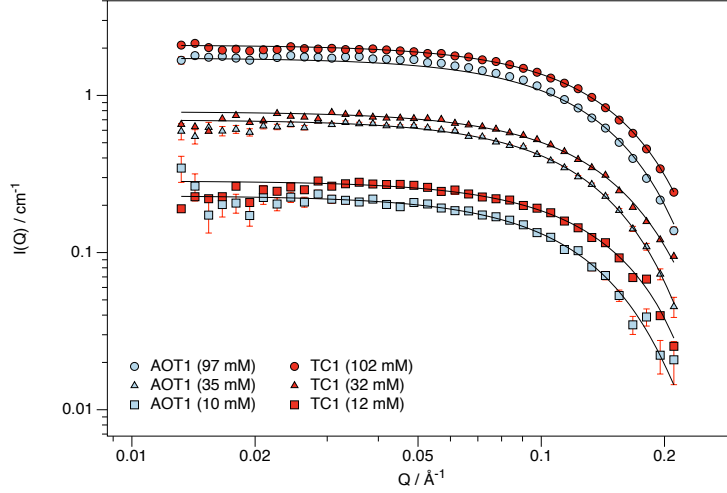


Figure 2: SANS of AOT1 and TC1 solutions in dodecane- $d_{26}$  as a function of concentration. The SANS curves are all qualitatively similar, and they can be fit to a spherical form factor with no dispersity. The mean size of the AOT1 inverse micelles ( $r \approx 16.0 \text{ \AA}$ ) is slightly larger than the mean size of the TC1 inverse micelles ( $r \approx 14.6 \text{ \AA}$ ).

$\sim 15 \text{ \AA}$ . This difference is small and insignificant in comparison to the Bjerrum length of dodecane ( $\lambda_B = 28 \text{ nm}$ ).

The difference in both the surfactant molecular volumes (TC1 greater than AOT1) and the inverse micelle radii (AOT1 greater than TC1) has an effect on the properties of the aggregates. In addition to the SANS fitting parameters, the aggregation number of the surfactant ( $n_{agg}$ ) and the number concentration of inverse micelles ( $n_i$ ) were calculated. The aggregation number ( $n_{agg}$ ) is determined by dividing the inverse micelle volume by the molecular volume (determined from the density and the molar mass;  $653 \text{ \AA}^3$  for AOT1 and  $903 \text{ \AA}^3$  for TC1). TC1 is assumed to have the same density as AOT1 for this calculation. Values of  $n_{agg}$  for AOT1 are consistent with those determined from other SANS measurements in alkanes.<sup>47</sup>  $n_{agg}$  for TC1 ( $\sim 15$ ) is much less, nearly half, than that of AOT1 ( $\sim 26$ ). This is expected given the larger molecular volume of TC1; the additional tail in TC1 means that it can cover the polar core with fewer surfactant molecules. The shape and approximate size of the inverse micelles are fixed due the curvature of the interface, and the larger TC1 surfactant can meet these requirements with fewer molecules. The number concentration

( $n_{IM}$ ) is determined by dividing the surfactant volume fraction by the volume of a single inverse micelle.  $n_{IM}$  of TC1 at each surfactant concentration is nearly twice that of AOT1. This is due the larger mass of TC1 in equimolar samples (due to its larger molar mass) as well as the smaller inverse micelle size.

The increased number concentration of inverse micelles is a possible origin of the increased charging ability of TC1 over AOT1. The ratio of the size of AOT1 and TC1 inverse micelles to  $\lambda_B$  is essentially the same, so energetically there should be little difference in the ability of the inverse micelles to stabilize charge. The number concentration of TC1 inverse micelles, however, is greater than of AOT1 inverse micelles. With a much larger number of counterions, dissociation of ions from the particles should be greater.

### ~~Ion dissociation~~ Proton affinity

The propensity for ion dissociation has an influence on both the conductivity of solutions and the charge of particles. Increased surfactant dissociation would result in a higher fraction of inverse micelles being charged and would encourage the dissociation of  $\text{Na}^+$  cations from latexes, resulting in a greater charge. Ion dissociation was studied by comparing the proton affinities for the two surfactants in their acid form. The proton affinity ( $E_{PA}$ ) is defined as the negative energy change of the reaction between a proton and a chemical species, shown below.<sup>48</sup>



The energies of the species studied were a sum of the electronic energy and the zero-point vibrational energy. DFT calculations were used to calculate the proton affinities for analogues of the two surfactants. Izgorodina *et al.* have shown that computational chemistry calculated proton affinities provide a useful scale for determining the delocalization of charge.<sup>22</sup>

Due to the large number of constituent atoms, performing computational chemistry calculations on surfactant molecules is computationally challenging. Therefore, it was preferable to compare the  $E_{PA}$  of the simplest possible analogues of the AOT1 and TC1 surfactants,

those with a methyl group as the tail. Using the convention for straight-chain surfactants,<sup>8,28</sup> the surfactants are referred to as di-C1SS (AOT1 analogue) and tri-C1SC (TC1 analogue).  $E_{PA}$  was calculated for AOT1 to compare to di-C1SS to see if this approximation was acceptable.

The values of  $E_{PA}$  for AOT1 (604.2 kJ mol<sup>-1</sup>) and di-C1SS (605.6 kJ mol<sup>-1</sup>) compare favorably, and they are equal within chemical accuracy (1 kcal mol<sup>-1</sup>  $\equiv$  4.184 kJ mol<sup>-1</sup>).<sup>22</sup>  $E_{PA}$  for tri-C1SC (599.8 kJ mol<sup>-1</sup>) is slightly smaller than for di-C1SS, above this threshold for chemical accuracy. However, the difference is small, and this seems unlikely to be the origin of the enhanced charging ability of TC1 surfactant.

### Electrical conductivity

The electrical conductivity of electrolyte solutions is related to the dissociation of surfactant ions, but it also depends on properties of the inverse micelles. Their size, the aggregation number, and the Coulomb energy required to charge them will all influence the conductivity. Electrical conductivity measurements can serve as an indicator of ion dissociation. However, they also enable determination of the strength of ion screening and the thickness of the double layer (the Debye length,  $\kappa^{-1}$ ). The relationship between the  $\zeta$  potential of a charged particle and its electrophoretic mobility depends on the magnitude of  $\kappa r$ .

The conductivity of surfactant solutions is a summation of all ionized species in solution (surfactant monomers and surfactant inverse micelles). However, CMCs for inverse micelle formation in organic solvents are very low ( $\sim 0.1$  mM for AOT1 in cyclohexane or dodecane).<sup>47</sup> Therefore, the concentration of monomers is less than the concentration of inverse micelles, and inverse micelles will be the primary charge carriers. Previous measurements of the conductivity of AOT in alkane solvents show that this assumption is appropriate. The conductivity of AOT monomers is several orders of magnitude lower than that of inverse micelles and can be excluded at concentrations above  $\sim 0.1$  mM.<sup>36,42,49</sup> The fraction of ionized inverse micelles ( $\chi$ ) can be calculated using Eicke's fluctuation theory for water-in-oil



microemulsions,<sup>50</sup> and the product of the conductivity and viscosity ( $\sigma\eta$ ) is proportional to the volume fraction ( $\phi$ ).<sup>40</sup>

The conductivities of AOT1 and TC1 solutions were measured at concentrations from 1–100 mM ( $\gg CMC$ ), and the results are shown in Figure 3. The conductivity of TC1 solutions are found to be lower than equimolar AOT1 solutions. The data in Figure 3 have been fit using fluctuation theory to determine the fraction of ionized inverse micelles. The radii and aggregation numbers used for the calculation were an average of the values at all concentrations. The fit values of  $\chi$  were found to be  $(1.3 \pm 0.2) \times 10^{-5}$  for AOT1 and  $(3.9 \pm 0.5) \times 10^{-6}$  for TC1. For reference, literature values for AOT1 in alkanes are  $\sim 10^{-5}$ .<sup>36,37,40,49</sup> This scales with the measured conductivity, as TC1 is less likely to dissociate than AOT1 and thus the conductivity is lower.

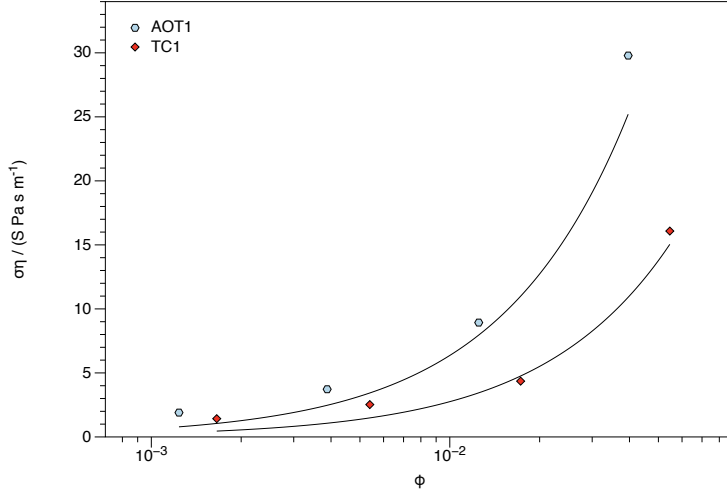



Figure 3: Conductivity of AOT1 and TC1 solutions in dodecane. From the slope of a plot of  $\sigma\eta$  as a function of  $\phi$ , it is possible to determine the fraction of ionized inverse micelles ( $\chi$ ). The value of  $\chi$  is  $(1.3 \pm 0.2) \times 10^{-5}$  for AOT1 and  $\chi$  is  $(3.9 \pm 0.5) \times 10^{-6}$  for TC1. Both the conductivity and degree of ionization of AOT1 are greater than for TC1.

The conductivity results can be understood by considering the properties of the surfactants discussed in the previous two sections. The values of  $E_{PA}$  for the two surfactants are effectively equal, and therefore, the likelihood of charge dissociation for an individual surfactant molecule is approximately the same. However, the values of  $n_{agg}$  for the two surfactants

are very different, with more AOT1 molecules in an inverse micelle. Therefore, an AOT1 inverse micelle contains more species with the potential to dissociate, leading to a larger number of charge carriers and a higher conductivity.

### **Electrokinetic or $\zeta$ potential**

The normalized electrophoretic mobilities ( $\mu/\mu_0$ ) of MC1 latexes charged by all AOTx and TCx surfactants were shown in Figure 1. Having measured the conductivities of AOT1 and TC1 solutions, the Debye lengths ( $\kappa^{-1}$ ) for these surfactant solutions are known, and it is possible to convert  $\mu$  into  $\zeta$  potentials. Three latexes of different sizes were studied at a volume fraction  $\phi = 5 \times 10^{-4}$  as a function of surfactant concentration. The value of  $r$  used for the calculations is the polymer core radius: the solvodynamic radius with the thickness of the PHS  steric layer (10 nm)<sup>51</sup> subtracted.

Two methods were used to determine the  $\zeta$  potential of the particles. For the larger latexes (MC1 and SF1), the magnitude of the  $\zeta$  potentials are great enough ( $> 50$  mV) that the Henry equation underestimates the potential, and the O'Brien and White method needs to be used.<sup>52,53</sup> For the smaller latex (GS1), the magnitude of the  $\zeta$  potential is lower, consistent with literature on small particles,<sup>2,36</sup> but the number concentration of particles is great and double layers begin to overlap. The Henry equation does not account for this, and Ohshima's expression accounting for overlapping double layers is used.<sup>54</sup> The calculated potentials for the three latexes are shown in Figure 4.

Unlike the magnitude of the electrophoretic mobility, which increases with decreasing surfactant concentration, the  $\zeta$  potential is independent of concentration. Depending on the latex, the magnitude of the  $\zeta$  potential is 25–60% greater for TC1 than AOT1. In fact, the low conductivity of TC1 means that the differences in the particle charge are actually underestimated by considering the electrophoretic mobility; the  $\zeta$  potentials of TC1 charged latexes are much greater than those of AOT1 charged latexes. A consideration of  $\zeta$  potentials, therefore, does not provide a possible explanation for the enhanced charging

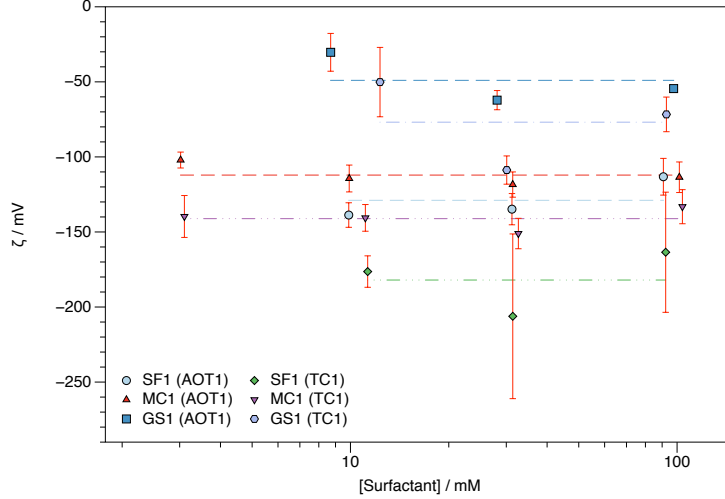


Figure 4:  $\zeta$  potentials of SF1, MC1, and GS1 latexes charged by AOT1 and TC1 in dodecane as a function of concentration measured by PALS. The particle concentration ( $\phi$ ) for PALS measurements was kept constant at  $5 \times 10^{-4}$ . PALS mobilities were converted into  $\zeta$  using either the O'Brien and White method (SF1 and MC1)<sup>53</sup> or Ohshima's expression for concentrated dispersions (GS1). The average value for each set is shown, as the latexes are assumed to have a constant potential independent of concentration.<sup>36,40,42</sup> For all particles, TC1 (dot-dash lines) introduces a larger magnitude potential than AOT1 (dash lines), consistent with the comparison of the electrophoretic mobilities alone.

ability of TCx surfactants. However, it does show that latexes are more highly charged by TCx surfactants than by AOTx surfactants and that the effective charge appears to be independent of surfactant concentration. This is because both methods used to the conversion from  $\mu$  to  $\zeta$  accounts for differences in the ionic background. The increased electrophoretic mobility at low surfactant concentrations (Figure 1) is not due to an increased effective charge on the particle but, rather, is due to the increased Debye layer thickness.

### CV-SANS Surfactant partitioning

The interaction of surfactants with PMMA latexes was studied using CV-SANS with deuterium-labeled surfactants. This approach has previously been used to study the interaction of PMMA latexes and AOT- $d_{34}$ ,<sup>14,36,46</sup> but the interaction of latexes with a new charging agent can now be studied as a result of the synthesis a new deuterium-labeled surfactant (TC1- $d_{31}$ ).

Due to the requirements of SANS measurements, small GS1 PMMA latexes ( $r = 38 \text{ \AA}$ ) have been used at a greater volume fraction ( $\phi = 0.02$ ) than used for PALS measurements. The electrokinetic properties of the GS1 particles have been measured for AOT1 and TC1 charged latexes in  $\sim 100 \text{ mM}$  surfactant solutions. The latexes are slightly negatively charged by both surfactants (AOT1— $\mu/\mu_0 = -0.19 \pm 0.14$ ,  $\zeta = -32 \pm 24 \text{ mV}$ ,  $Z = -1.2 \pm 0.9e$ ; TC1— $\mu/\mu_0 = -0.12 \pm 0.23$ ,  $\zeta = -34 \pm 66 \text{ mV}$ ,  $Z = -1.3 \pm 2.5e$ ), although the error for the TC1 charged latex is greater than the magnitude of the potential. The resolution of the charge of these latexes is low because the electrophoretic mobility of concentrated dispersions of small particles is retarded due to the double layer overlap.<sup>54</sup> However, it is reasonable to assume that the particles have a slight negative charge in agreement with literature.<sup>36–38,40</sup>

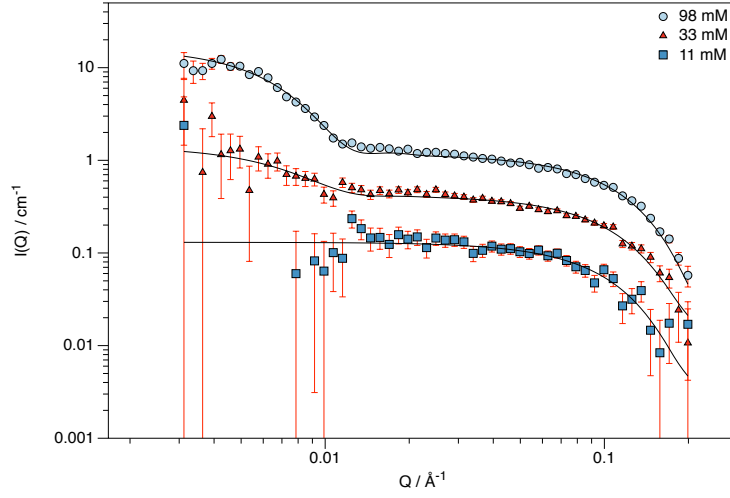
**~~Latex only SANS.~~ Latex scattering.** As the latexes are composite particles consisting of multiple monomers and other species,<sup>15</sup> the scattering length density ( $\rho$ ) of the latexes should be determined experimentally rather than computationally (shown in Supporting Information). The GS1 latexes are found to have a SLD of  $\rho = 1.1 \times 10^{-6} \text{ \AA}^{-2}$ . This is essentially the same as for the DG1 latexes used by Smith *et al.* ( $\rho = 1.0 \times 10^{-6} \text{ \AA}^{-2}$ )<sup>14</sup> but is greater than the RK2 latexes used by Kemp *et al.* ( $\rho = 0.11 \times 10^{-6} \text{ \AA}^{-2}$ ). The amount of residual scattering of GS1 latexes was found to be negligible, and the small amount of scattering can be attributed to a small contribution from the PHS polymer.<sup>55</sup> The residual scattering curve was fit to a core-shell model with scattering arising from the latex shell and then subtracted from all CV-SANS curves.

**~~Latex and AOT1- $d_{34}$  and TC1- $d_{51}$  CV-SANS.~~ AOT1- $d_{34}$  and TC1- $d_{51}$  scattering.** The interaction of AOT with charged particles in nonpolar solvents is often described as the adsorption of inverse micelles or hemimicelles.<sup>56–59</sup> CV-SANS studies of the interaction of AOT with PMMA latexes have shown that the surfactant interacts with the particles without a preferential morphology rather than as inverse micellar aggregates.<sup>14,36,46</sup> Smith *et al.* showed that a shell-scattering model was found to poorly agree with the CV-SANS of

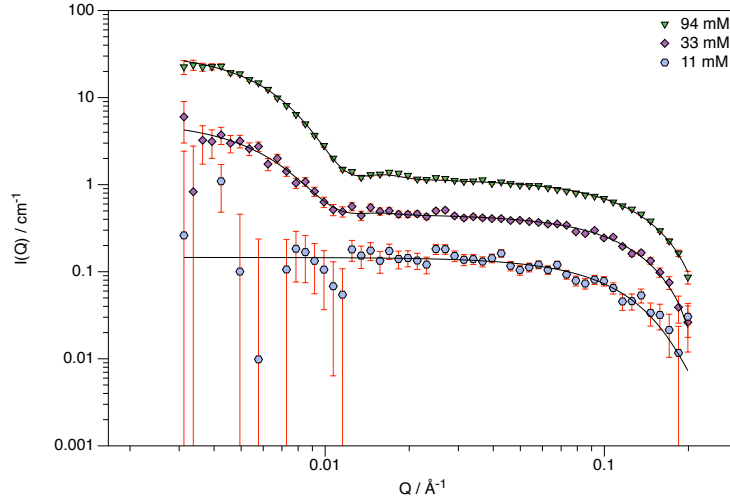
AOT- $d_{34}$  with on DG1 latexes,<sup>14</sup> and this is also the case for GS1 latexes with AOT1- $d_{34}$  and TC1- $d_{51}$  (shown in Supporting Information). The extensive CV-SANS experiments presented in that study showed that the surfactant can be considered to be located throughout the entire latex.<sup>14</sup> In this model, the interaction of surfactants with the PMMA latexes is not the typical “adsorption” used to describe surface interactions and should be thought of as “absorption” into the PMMA cores.<sup>46</sup> This is the only model that can be used to successfully model the CV-SANS data. Consequently, the interaction of surfactants with the PMMA cores is more significant than the interaction of AOT with the PHSA shells. ~~The same model is used to fit the data in this study; the~~ In this study, the total scattering is modeled as a sum of small inverse micelle spheres ( $\sim 20$  Å) and large absorbed surfactant-in-latex core-shell spheres ( $\sim 300$  Å). Unlike in the previous study, the radius of the latex core is allowed to vary to obtain the best fit to the data, but this difference is less than the thickness of the stabilizer shell. This difference is not inconsistent with the previous study. The data cannot be fit if the surfactant is assumed to locate only in the stabilizer shell; it must be distributed throughout the whole of the latex.

The CV-SANS curves of AOT1- $d_{34}$  and TC1- $d_{51}$  surfactants with GS1 latexes ( $\phi = 0.02$ ) in dodecane are shown in Figures 5. Only samples with  $\sim 100$  or  $\sim 32$  mM concentrations of surfactant show detectable scattering above the inverse micellar background and the residual latex scattering; the most dilute solutions do not show scattering above the backgrounds. The amount of surfactant absorbed into the latexes is known to vary with solution concentration,<sup>14</sup> and these measurements are consistent with that observation. The three surfactant concentrations studied are logarithmically spaced, and the intensity of the scattering curves are evenly spaced on log-log axes. This shows that the amount of surfactant located both in inverse micelles and in the latexes scales with the total concentration of surfactant.

The fit inverse micelle radii from these CV-SANS measurements are slightly greater than the measurements performed on unlabeled surfactant in dodecane- $d_{26}$ , consistent with





(a) AOT1- $d_{34}$



(b) TC1- $d_{51}$

Figure 5: CV-SANS of AOT1- $d_{34}$  (5a) and TC1- $d_{51}$  (5b) with GS1 latexes ( $\phi = 0.02$ ) in CM-dodecane at three surfactant concentrations. The curves are fit as a sum of inverse micelle spheres and absorbed surfactant-in-latex core-shell spheres, which is a good description of the curves across the whole  $Q$ -range. The scattering at low- $Q$  from absorbed TC1- $d_{51}$  is greater than AOT1- $d_{34}$ .

literature, where the inverse micelles from the fit CV-SANS data were found to be larger than from unlabelled surfactant.<sup>14</sup> The differences in size are slight (a few Å), and the analytical chemistry agrees with the predicted structure. The difference is likely due to the reduced contrast that comes from using deuterium-labeled surfactants in CM-solvent ( $I(Q) \propto \Delta\rho^2$ ).

Variation of the core radius was not necessary to model previous data,<sup>14</sup> but it is required to fit the CV-SANS of GS1 latexes in this study, although the difference from expected size is slight. In the CV-SANS measurements on GS1 latexes in Figure 5, the PMMA latexes were completely contrast matched, and only the cture of the deuterium-labeled surfactant core be determined. SAXS measurements were also performed on AOT1 containing latexes (shown in Supporting Information), and these data are sensitive to the particle core only and insensitive to the surfactant or polymer stabilizer. The radii of latexes both with and without AOT1 are essentially the same, demonstrating that the presence of the surfactant does not modify the latex significantly and that the differences in the fit size are due to resolution of data fitting.

**~~Analysis of surfactant~~ Equilibrium partitioning.** From the contrast between particle and solvent ( $\Delta\rho$ ), the amount of surfactant present in the latexes can be estimated. From a simple analysis, there is more deuterium-labeled material in latexes charged by TC1- $d_{51}$  as  $\Delta\rho$  is greater than for AOT- $d_{34}$ . However, the SLD of TC1- $d_{51}$  is also greater than that of AOT1- $d_{34}$ , as it has more D nuclei per unit volume, so a greater  $\Delta\rho$  does not necessarily mean that a greater number of surfactant molecules are incorporated.

More complex analysis can be performed by using the CV-SANS results to determine the partitioning of surfactant from the inverse micelles to the latexes. The magnitude of  $\Delta\rho$  can be used to estimate the volume fraction of surfactant absorbed in the particles ( $\Delta\rho/\rho_{\text{surfactant}}$ ), and the total volume fraction of surfactant in the particles is the product of the particle volume fraction and this value ( $\phi_b = \phi_{\text{GS1}} \cdot \Delta\rho/\rho_{\text{surfactant}}$ ). It is possible to convert this to the number concentration of surfactant molecules in the latex ( $n_i$ ) using the

molecular volume of the surfactants. The volume fraction of surfactant present as inverse micelles ( $\phi_{IM}$ ) is equal to the fit scale factor.

Using the values of  $\phi_b$  and  $\phi_{IM}$ , it is possible to estimate the equilibrium constant  $K_b$  between surfactant in the inverse micellar and bound phases, shown in Equations 2 and 3, using the law of mass action. The surfactant concentrations are much greater than the CMC for inverse micelle formation,<sup>47</sup> and the total amount of surfactant is assumed to be a sum of two populations ( $[\text{Surfactant}]_{IM}$  and  $[\text{Surfactant}]_b$ ).

$$[\text{Surfactant}]_{IM} \rightleftharpoons [\text{Surfactant}]_b \quad (2)$$

$$K_b = \frac{[\text{Surfactant}]_b}{[\text{Surfactant}]_{IM}} \quad (3)$$

From the values of  $K_b$ , it is possible to estimate the free energy change of surfactant adsorbing into the latexes ( $\Delta G_b$ ) from the relationship,  $\Delta G = -RT \ln(K)$ . The values of  $\phi_{IM}$ ,  $\phi_b$ ,  $K_b$ , and  $\Delta G_b$  are shown in Table 3. Data for the most dilute surfactant solutions are not shown; using the value for  $K_b$ , the  $\Delta\rho$  for these systems was calculated to be  $0.02 \times 10^{-6} \text{ \AA}^{-2}$ , below instrumental resolution. While the amount of absorbed surfactant is different at different concentrations, the value of  $K_b$  and  $\Delta G_b$  is identical.

Table 3: Partitioning of AOT1- $d_{34}$  and TC1- $d_{51}$  into GS1 latexes ( $\phi_b$ ,  $K_b$ , and  $\Delta G_b$ ) from CV-SANS measurements.

$[\text{AOT1-}d_{34}] / \text{mM}$	$\phi_{IM}/10^{-2}$	$\phi_b / 10^{-3}$	$n_i / (10^{24} \text{ m}^{-3})$	$K_b$	$\Delta G_b / RT$
98	1.98	1.18	1.80	0.0593	3.02
33	0.622	0.366	0.560	0.0588	3.02
$[\text{TC1-}d_{34}] / \text{mM}$	$\phi_{IM}/10^{-2}$	$\phi_b / 10^{-3}$	$n_i / (10^{24} \text{ m}^{-3})$	$K_b$	$\Delta G_b / RT$
94	3.39	1.436	1.58	0.0421	3.39
33	1.31	0.544	0.603	0.0417	3.38

An examination of the equilibrium partitioning of surfactant shows that the system is more complex than a simple consideration of  $\Delta\rho$  would suggest. The contrast between the



deuterium-labeled material located in the GS1 latexes is greater for TC1- $d_{51}$  than AOT1- $d_{34}$ . The free energy of transferring surfactant from inverse micelles to particles, however, is very similar for the two charging agents. In fact, the difference between the two would suggest that more AOT1- $d_{34}$  partitions into the latexes than TC1- $d_{51}$ , which is not consistent with TC1 being the more effective charging agent.

## Discussion

Several possible origins of the difference in charging ability of AOT1 and TC1 surfactants were proposed. This included differences in the surfactant molecules (ion dissociation), the surfactant aggregates in solution (inverse micelle size or conductivity), or the surfactant incorporated into the latexes ( $\zeta$  potential or amount of surfactant absorbed).

The degree of ion dissociation and inverse micelle radius are essentially the same for AOT1 and TC1 so cannot be the origin of the differing charging ability. The electrical conductivities of TC1 solutions are also less than of AOT1 solutions, which shows that TC1 is not more likely to charge dissociate. The amount of surfactant incorporated into the particles as well as the free energy of this equilibrium (measured by CV-SANS) are similar for the two surfactants.

The main differences between the two surfactants are related to the inverse micelles. This is not the sizes of the aggregates, which are effectively the same on the scale of  $\lambda_B$ . Rather, the aggregation number of TC1 is lower, and consequently, there are a much larger number concentration of inverse micelles. This results in more counterions to solubilize any disproportionated  $\text{Na}^+$  cations from the latexes, resulting in a larger effective charge.

As few systematic studies have been performed on varying the structure of surfactants as charge control agents, there are few similar reports to compare this too. However, Parent *et al.* have performed one of the few studies of the relationship between molecular variation and particle charge, and they studied modifications in the head group of polyisobutylene

succinimide analogues. They found that the charge of pigment particles was inversely proportional to the number of charged micelles in solution.<sup>60</sup> Despite these two studies being on completely different systems, the results suggest the same relationship between surfactant structure and properties. The more effective a surfactant is as an electrolyte, the less effective it seems to be as a charge control additive.

## Conclusions

Systematic variations have been made to the alkyl tails of AOT analogues to explore if changes in molecular structure have an effect on the electrophoretic mobility and charge of PMMA latexes. These variations are more subtle than have been attempted in the past where the differences have been comparing acidic or basic surfactants or comparing nonionic and anionic surfactants.<sup>1</sup>

Modifying the tail branching does not seem to have any effect on the particle charge. Varying the number of surfactant tails (from two to three) does seem to influence the particle charge, increasing both the electrophoretic mobility and the  $\zeta$  potential. Changing the number of surfactant tails changes the packing and hydrophobicity of the surfactant; a relationship between surfactant structure and particle charge has also recently been seen with nonionic surfactant charge control additives for mineral oxides.<sup>13</sup>

The most likely origin of the increased charging ability of TCx surfactants compared to AOTx surfactants is that they form a larger number of inverse micelles. This is interesting because the same property of TC1 that makes it a poor microemulsifier (high film curvature leading to a large number of small droplets)<sup>11</sup> seems to be the same property that makes it a more effective charge control additive.

These results suggest that a successful strategy for developing effective charge control additives is to produce molecules that strongly interact with particles, that produce a large number concentration of inverse micelles, and that do not result in greater electrical con-

ductivities, but these criteria may be difficult to balance in practice. Comparing TC1 and AOT1 as charge control additives has shown that simple molecular variations do have an effect on the electrophoretic mobility and electrokinetic potential of particles, and this is an avenue that warrants further research.

## Acknowledgement

GNS acknowledges Merck Chemicals Ltd. UK, an affiliate of Merck KGaA, Darmstadt, Germany, and the UK Engineering and Physical Sciences Research Council (EPSRC) for the provision of a CASE PhD studentship. The authors thank the UK Science and Technology Facilities Council (STFC) for allocation of beamtime at ISIS and grants toward consumables and travel. The authors thank Diamond Light Source for provision of beamtime on I22 and travel funding. Olga Shebanova (Diamond) as well as Jocelyn Peach and David A. J. Gillespie (Bristol) are acknowledged for assistance on I22. This work benefitted from SasView software, originally developed by the DANSE project under NSF award DMR-0520547.

## References

- (1) Smith, G. N.; Eastoe, J. Controlling colloid charge in nonpolar liquids with surfactants. *Phys. Chem. Chem. Phys.* **2013**, *15*, 424–439.
- (2) Smith, G. N.; Hallett, J. E.; Eastoe, J. Celebrating *Soft Matter*’s 10th Anniversary: Influencing the charge of poly(methyl methacrylate) latexes in nonpolar solvents. *Soft Matter* **2015**, *11*, 8029–8041.
- (3) Morrison, I. D. Electrical charges in nonaqueous media. *Colloids Surf. A: Physicochem. Eng. Aspects* **1993**, *71*, 1–37.
- (4) Klinkenberg, A., van der Minne, J. L., Eds. *Electrostatics in the Petroleum Industry: The Prevention of Explosion Hazards*; Elsevier: London, 1958.

- (5) Croucher, M. D.; Lok, K. P.; Wong, R. W.; Drappel, S.; Duff, J. M.; Pundsack, A. L.; Hair, M. L. Use of sterically stabilized polymer colloids as electrostatically-based liquid developers. *J. Appl. Polym. Sci.* **1985**, *30*, 593–607.
- (6) Ota, I.; Ohnishi, J.; Yoshiyama, M. Electrophoretic image display (EPID) panel. *Proc. IEEE* **1973**, *61*, 832–836.
- (7) Comiskey, B.; Albert, J. D.; Yoshizawa, H.; Jacobson, J. An electrophoretic ink for all-printed reflective electronic displays. *Nature* **1998**, *394*, 253–255.
- (8) Nave, S.; Eastoe, J.; Heenan, R. K.; Steytler, D.; Grillo, I. What Is So Special about Aerosol-OT? 2. Microemulsion Systems. *Langmuir* **2000**, *16*, 8741–8748.
- (9) Hollamby, M. J.; Trickett, K.; Mohamed, A.; Cummings, S.; Tabor, R. F.; Myakonkaya, O.; Gold, S.; Rogers, S.; Heenan, R. K.; Eastoe, J. Tri-Chain Hydrocarbon Surfactants as Designed Micellar Modifiers for Supercritical CO<sub>2</sub>. *Angew. Chem. Int. Ed.* **2009**, *48*, 4993–4995.
- (10) Mohamed, A.; Trickett, K.; Chin, S. Y.; Cummings, S.; Sagisaka, M.; Hudson, L.; Nave, S.; Dyer, R.; Rogers, S. E.; Heenan, R. K.; Eastoe, J. Universal Surfactant for Water, Oils, and CO<sub>2</sub>. *Langmuir* **2010**, *26*, 13861–13866.
- (11) Hudson, L. K. Structure versus Performance Surfactants at Interfaces. Ph.D. thesis, University of Bristol, 2008.
- (12) Israelachvili, J. N.; Mitchell, D. J.; Ninham, B. W. Theory of self-assembly of hydrocarbon amphiphiles into micelles and bilayers. *J. Chem. Soc., Faraday Trans. 2* **1976**, *72*, 1525–1568.
- (13) Gacek, M. M.; Berg, J. C. Effect of surfactant hydrophile-lipophile balance (HLB) value on mineral oxide charging in apolar media. *J. Colloid Interface Sci.* **2014**,

- (14) Smith, G. N.; Alexander, S.; Brown, P.; Gillespie, D. A. J.; Grillo, I.; Heenan, R. K.; James, C.; Kemp, R.; Rogers, S. E.; Eastoe, J. Interaction between Surfactants and Colloidal Latexes in Nonpolar Solvents Studied Using Contrast-Variation Small-Angle Neutron Scattering. *Langmuir* **2014**, *30*, 3422–3431.
- (15) Antl, L.; Goodwin, J. W.; Hill, R. D.; Ottewill, R. H.; Owens, S. M.; Papworth, S.; Waters, J. A. The preparation of poly(methyl methacrylate) latices in non-aqueous media. *Colloids Surf.* **1986**, *17*, 67–78.
- (16) Heenan, R. K.; Rogers, S. E.; Turner, D.; Terry, A. E.; Treadgold, J.; King, S. M. Small Angle Neutron Scattering Using Sans2d. *Neutron News* **2011**, *22*, 19–21.
- (17) Heenan, R. K.; Penfold, J.; King, S. M. SANS at Pulsed Neutron Sources: Present and Future Prospects. *J. Appl. Cryst.* **1997**, *30*, 1140–1147.
- (18) Wignall, G. D.; Bates, F. S. Absolute Calibration of Small-Angle Neutron Scattering Data. *J. Appl. Cryst.* **1987**, *20*, 28–40.
- (19) Gillespie, D. A. J.; Hallett, J. E.; Elujoba, O.; Che Hamzah, A. F.; Richardson, R. M.; Bartlett, P. Counterion condensation on spheres in the salt-free limit. *Soft Matter* **2014**, *10*, 566–577.
- (20) Frisch, M. J. et al. Gaussian 09 Revision D.01. Gaussian Inc. Wallingford CT 2009.
- (21) Scott, A. P.; Radom, L. Harmonic Vibrational Frequencies: An Evaluation of Hartree–Fock, Møller–Plesset, Quadratic Configuration Interaction, Density Functional Theory, and Semiempirical Scale Factors. *J. Phys. Chem.* **1996**, *100*, 16502–16513.
- (22) Izgorodina, E. I.; Forsyth, M.; MacFarlane, D. R. Towards a Better Understanding of ‘Delocalized Charge’ in Ionic Liquid Anions. *Aust. J. Chem.* **2007**, *60*, 15–20.
- (23) Israelachvili, J. The science and applications of emulsions—an overview. *Colloids Surf. A: Physicochem. Eng. Aspects* **1994**, *91*, 1–8.

- (24) Pitt, A. In *Amphiphiles at Interfaces*; Texter, J., Ed.; Prog. Colloid Polym. Sci.; Steinkopff, 1997; Vol. 103; pp 307–317.
- (25) Leydet, A.; Boyer, B.; Lamaty, G.; Roque, J. P.; Catlin, K.; Menger, F. M. Nitrogen Analogs of AOT. Synthesis and Properties. *Langmuir* **1994**, *10*, 1000–1002.
- (26) Tanford, C. *The Hydrophobic Effect: Formation of Micelles and Biological Membranes*, 2nd ed.; John Wiley & Sons: Chichester, 1980.
- (27) Rosen, M. J.; Wang, H.; Shen, P.; Zhu, Y. Ultralow Interfacial Tension for Enhanced Oil Recovery at Very Low Surfactant Concentrations. *Langmuir* **2005**, *21*, 3749–3756.
- (28) Nave, S.; Eastoe, J.; Penfold, J. What Is So Special about Aerosol-OT? 1. Aqueous Systems. *Langmuir* **2000**, *16*, 8733–8740.
- (29) Nave, S. Phase behaviour and interfacial properties of double-chain anionic surfactants. Ph.D. thesis, University of Bristol, 2001.
- (30) Bjerrum, N. Untersuchungen Über Ionenassoziation. I. Der Einfluss der Ionenassoziation auf die Aktivität der Ionen bei Mittleren Assoziationsgraden. *Kgl. Danske Vidensk. Selsk., Mat.-fys. Medd.* **1926**, *7*, 1–48.
- (31) Einstein, A. Eine neue Bestimmung der Moleküldimensionen. *Ann. Phys.* **1906**, *324*, 289–306.
- (32) Einstein, A. Berichtigung zu meiner Arbeit: „Eine neue Bestimmung der Moleküldimensione“. *Ann. Phys.* **1911**, *339*, 591–592.
- (33) Roberts, G. S. Single Particle Optical Microelectrophoresis: Direct Measurement of Effective Charges in Nonaqueous Systems. Ph.D. thesis, University of Bristol, 2007.
- (34) Kotlarchyk, M.; Huang, J. S.; Chen, S.-H. Structure of AOT reversed micelles determined by small-angle neutron scattering. *J. Phys. Chem.* **1985**, *89*, 4382–4386.

- (35) Guinier, A.; Fournet, G. *Small-Angle Scattering of X-Rays*; John Wiley & Sons: New York, 1955.
- (36) Kemp, R.; Sanchez, R.; Mutch, K. J.; Bartlett, P. Nanoparticle Charge Control in Nonpolar Liquids: Insights from Small-Angle Neutron Scattering and Microelectrophoresis. *Langmuir* **2010**, *26*, 6967–6976.
- (37) Hsu, M. F.; Dufresne, E. R.; Weitz, D. A. Charge Stabilization in Nonpolar Solvents. *Langmuir* **2005**, *21*, 4881–4887.
- (38) Roberts, G. S.; Wood, T. A.; Frith, W. J.; Bartlett, P. Direct measurement of the effective charge in nonpolar suspensions by optical tracking of single particles. *J. Chem. Phys.* **2007**, *126*, 194503.
- (39) Sainis, S. K.; Germain, V.; Dufresne, E. R. Statistics of Particle Trajectories at Short Time Intervals Reveal fN-Scale Colloidal Forces. *Phys. Rev. Lett.* **2007**, *99*, 018303.
- (40) Roberts, G. S.; Sanchez, R.; Kemp, R.; Wood, T.; Bartlett, P. Electrostatic Charging of Nonpolar Colloids by Reverse Micelles. *Langmuir* **2008**, *24*, 6530–6541.
- (41) Wood, T. A.; Roberts, G. S.; Eaimkhong, S.; Bartlett, P. Characterization of microparticles with driven optical tweezers. *Faraday Discuss.* **2008**, *137*, 319–333.
- (42) Sainis, S. K.; Merrill, J. W.; Dufresne, E. R. Electrostatic Interactions of Colloidal Particles at Vanishing Ionic Strength. *Langmuir* **2008**, *24*, 13334–13337.
- (43) Sainis, S. K.; Germain, V.; Mejean, C. O.; Dufresne, E. R. Electrostatic Interactions of Colloidal Particles in Nonpolar Solvents: Role of Surface Chemistry and Charge Control Agents. *Langmuir* **2008**, *24*, 1160–1164.
- (44) Merrill, J. W.; Sainis, S. K.; Dufresne, E. R. Many-Body Electrostatic Forces between Colloidal Particles at Vanishing Ionic Strength. *Phys. Rev. Lett.* **2009**, *103*, 138301.

- (45) Merrill, J. W.; Sainis, S. K.; Blawdziewicz, J.; Dufresne, E. R. Many-body force and mobility measurements in colloidal systems. *Soft Matter* **2010**, *6*, 2187–2192.
- (46) Smith, G. N.; Grillo, I.; Rogers, S. E.; Eastoe, J. Surfactants with colloids: Adsorption or absorption? *J. Colloid Interface Sci.* **2015**, *449*, 205–214.
- (47) Smith, G. N.; Brown, P.; Rogers, S. E.; Eastoe, J. Evidence for a Critical Micelle Concentration of Surfactants in Hydrocarbon Solvents. *Langmuir* **2013**, *29*, 3252–3258.
- (48) Muller, P. Glossary of terms used in physical organic chemistry (IUPAC Recommendations 1994). *Pure Appl. Chem.* **1994**, *66*, 1077–1184.
- (49) Schmidt, J.; Prignitz, R.; Peschka, D.; Münch, A.; Wagner, B.; Bansch, E.; Peukert, W. Conductivity in nonpolar media: Experimental and numerical studies on sodium AOT–hexadecane, lecithin–hexadecane and aluminum(III)-3,5-diisopropyl salicylate–hexadecane systems. *J. Colloid Interface Sci.* **2012**, *386*, 240–251.
- (50) Eicke, H. F.; Borkovec, M.; Das-Gupta, B. Conductivity of water-in-oil microemulsions: a quantitative charge fluctuation model. *J. Phys. Chem.* **1989**, *93*, 314–317.
- (51) Cebula, D. J.; Goodwin, J. W.; Ottewill, R. H.; Jenkin, G.; Tabony, J. Small angle and quasi-elastic neutron scattering studies on polymethylmethacrylate latices in nonpolar media. *Colloid Polym. Sci.* **1983**, *261*, 555–564.
- (52) Delgado, A. V.; González-Caballero, F.; Hunter, R. J.; Koopal, L. K.; Lyklema, J. Measurement and Interpretation of Electrokinetic Phenomena (IUPAC Technical Report). *Pure Appl. Chem.* **2005**, *77*, 1753–1805.
- (53) O’Brien, R. W.; White, L. R. Electrophoretic mobility of a spherical colloidal particle. *J. Chem. Soc., Faraday Trans. 2* **1978**, *74*, 1607–1626.
- (54) Ohshima, H. Electrophoretic Mobility of Spherical Colloidal Particles in Concentrated Suspensions. *J. Colloid Interface Sci.* **1997**, *188*, 481–485.



- (55) Washington, A. L.; Li, X.; Schofield, A. B.; Hong, K.; Fitzsimmons, M. R.; Dalglish, R.; Pynn, R. Inter-particle correlations in a hard-sphere colloidal suspension with polymer additives investigated by Spin Echo Small Angle Neutron Scattering (SESANS). *Soft Matter* **2014**, *10*, 3016–3026.
- (56) Smith, P. G., Jr.; Patel, M. N.; Kim, J.; Milner, T. E.; Johnston, K. P. Effect of Surface Hydrophilicity on Charging Mechanism of Colloids in Low-Permittivity Solvents. *J. Phys. Chem. C* **2007**, *111*, 840–848.
- (57) Patel, M. N.; Smith, P. G., Jr.; Kim, J.; Milner, T. E.; Johnston, K. P. Electrophoretic mobility of concentrated carbon black dispersions in a low-permittivity solvent by optical coherence tomography. *J. Colloid Interface Sci.* **2010**, *345*, 194–199.
- (58) Cao, H.; Cheng, Y.; Huang, P.; Qi, M. Investigation of charging behavior of PS particles in nonpolar solvents. *Nanotechnology* **2011**, *22*, 445709.
- (59) Cao, H.; Lu, N.; Ding, B.; Qi, M. Regulation of charged reverse micelles on particle charging in nonpolar media. *Phys. Chem. Chem. Phys.* **2013**, *15*, 12227–12234.
- (60) Parent, M. E.; Yang, J.; Jeon, Y.; Toney, M. F.; Zhou, Z.-L.; Henze, D. Influence of Surfactant Structure on Reverse Micelle Size and Charge for Nonpolar Electrophoretic Inks. *Langmuir* **2011**, *27*, 11845–11851.

